

Chapter 2

Modeling of trees

Computer simulation of branching patterns has a relatively long history. The first model was proposed by Ulam [149], (see also [138, pages 127–131]), and employed the concept of *cellular automata* that had been developed earlier by von Neumann and Ulam [156]. The branching pattern is created iteratively, starting with a single colored cell in a triangular grid, then coloring cells that touch one and only one vertex of a cell colored in the previous iteration step.

Cellular-space models

This basic idea gave rise to several extensions. Meinhardt [97, Chapter 15] substituted the triangular grid with a square one, and used the resulting cellular space to examine biological hypotheses related to the formation of net-like structures. In addition to pure branching patterns, his models capture the effect of branch reconnection or *anastomosis* that may take place between the veins of a leaf. Greene [54] extended cellular automata to three dimensions, and applied the resulting *voxel space automata* to simulate growth processes that react to the environment. For instance, Figure 2.1 presents the growth of a vine over a house. Cohen [15] simulated the development of a branching pattern using expansion rules that operate in a continuous “density field” rather than a discrete cellular or voxel space.

The common feature of these approaches is the emphasis on interactions between various elements of a growing structure, as well as the structure and the environment. Although interactions clearly influence the development of real plants, they also add to the complexity of the models. This may explain why simpler models, ignoring even such fundamental factors as collisions between branches, have been prevalent to date. The first model in that category was proposed by Honda [65] who studied the form of trees using the following assumptions (Figure 2.2).

Honda’s model

- Tree segments are straight and their girth is not considered.
- A mother segment produces two daughter segments through one branching process.



Figure 2.1: *Organic architecture* by Greene [54]

- The lengths of the two daughter segments are shortened by constant ratios, r_1 and r_2 , with respect to the mother segment.
- The mother segment and its two daughter segments are contained in the same *branch plane*. The daughter segments form constant *branching angles*, a_1 and a_2 , with respect to the mother branch.
- The branch plane is fixed with respect to the direction of gravity so as to be closest to a horizontal plane.¹ An exception is made for branches attached to the main trunk. In this case, a constant *divergence angle* α between consecutively issued lateral segments is maintained (cf. Chapter 4).

By changing numerical parameters, Honda obtained a wide variety of tree-like shapes. With some improvements [38], his model was applied to investigate branching patterns of real trees [39, 66, 67, 68]. Subsequently, different rules for branching angles were proposed to capture the structure of trees in which planes of successive bifurcations are perpendicular to each other [69]. The results of Honda served as a basis for the tree models proposed by Aono and Kunii [2]. They suggested

¹More formally, the line perpendicular to the mother segment and lying in the branch plane is horizontal.

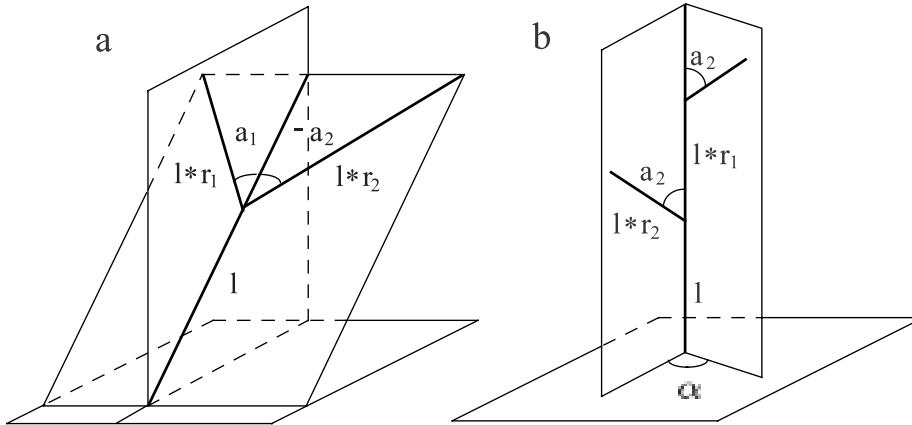


Figure 2.2: Specification of tree geometry according to Honda [65]

several extensions to his model, the most important of which was the biasing of branch positions in a particular direction, applied to produce the effects of wind, phototropism and gravity. A similar concept was introduced previously by Cohen [15], while more accurate physically-based methods for branch bending were developed by de Reffye [28] and Armstrong [4].

The models of Honda and Aono and Kunii were rendered using straight lines of constant or varying width to represent “tree skeletons.” A substantial improvement in the realism of synthetic images was achieved by Bloomenthal [11] and Oppenheimer [105], who introduced curved branches, carefully modeled surfaces around branching points, and textured bark and leaves (Figure 2.3).

The approaches stemming from the work of Honda defined branching structures using deterministic algorithms. In contrast, stochastic mechanisms are essential to the group of tree models proposed by Reeves and Blau [119], de Reffye *et al.* [30], and Remphrey, Neal and Steeves [120]. Although these models were described using different terminologies, they share the basic paradigm of specifying tree structures in terms of probabilities with which branches are formed. The work of Reeves and Blau aimed at producing tree-like shapes without delving into biological details of the modeled structures (Figure 2.4). In contrast, de Reffye *et al.* [29] used a stochastic approach to simulate the development of real plants by modeling the activity of buds at discrete time intervals. Given a clock signal, a bud can either:

- do nothing,
- become a flower,
- become an internode terminated by a new straight apex and one or more lateral apices subtended by leaves, or
- die and disappear.

Realism

Stochastic models

Approach of de Reffye

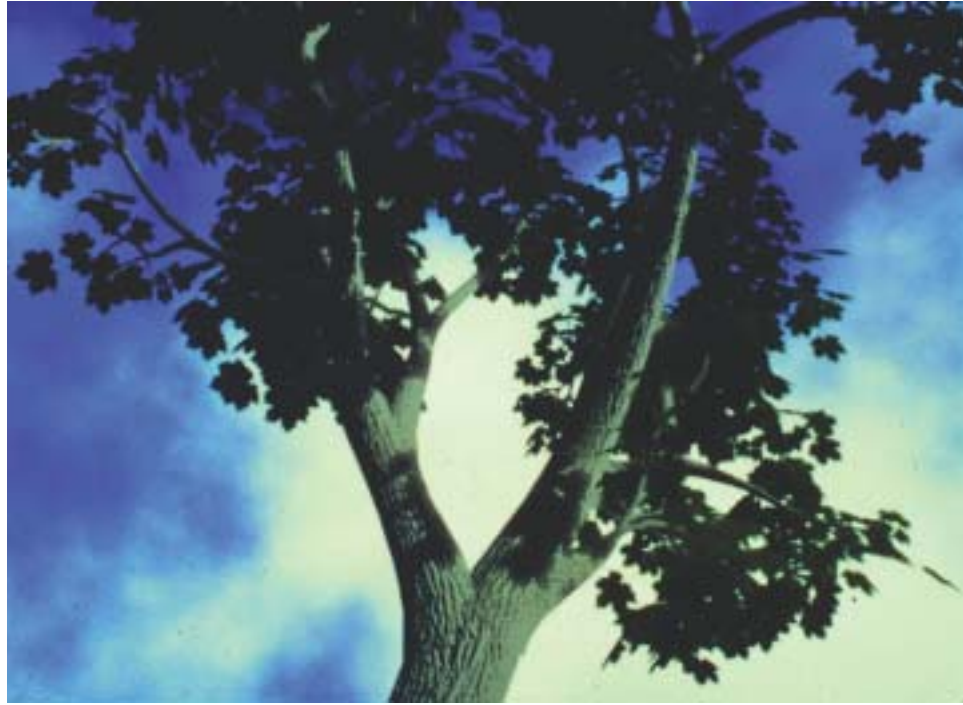


Figure 2.3: *Acer graphics* by Bloomenthal [11]



Figure 2.4: A forest scene by Reeves [119] ©1984 Pixar



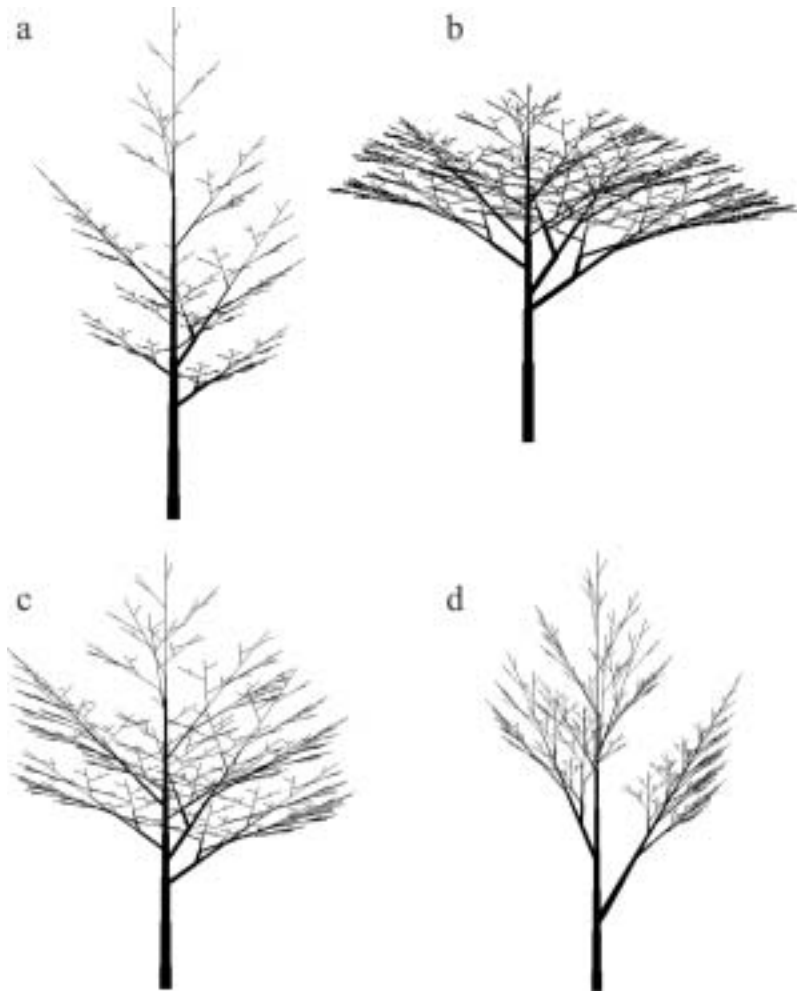
Figure 2.5: Oil palm tree canopy from CIRAD Modelisation Laboratory

These events occur according to stochastic laws characteristic for each variety and each species. The geometric parameters, such as the length and diameter of an internode, as well as branching angles, are also calculated according to stochastic laws.

The basic types of developmental rules incorporated into this method correspond to the 23 different types of tree architectures identified by Hallé, Oldeman and Tomlinson [58]. Detailed models of selected plant species were developed and are described in the literature [16, 20, 26, 27, 76]. A sample tree model is shown in Figure 2.5. The approach of Remphrey [120, 121, 122] is similar to that of de Reffye, except that larger time steps are used (one year in the model of bearberry described in [120]). Consequently, the stochastic rules must describe the entire configuration of lateral shoots that can be formed over a one-year period.

The application of L-systems to the generation of botanical trees was first considered by Aono and Kunii [2]. They referred to the original definition of L-systems [82] and found them unsuitable to model the complex branching patterns of higher plants. However, their arguments do not extend to parametric L-systems with turtle interpretation. For example, the L-system in Figure 2.6 implements those tree models of Honda [65] in which one of the branching angles is equal to 0, yielding a *monopodial* structure with clearly delineated main and lateral axes (see Section 3.2 for a formal characterization).

*Application of
L-systems*



```

n = 10
#define r1 0.9    /* contraction ratio for the trunk */
#define r2 0.6    /* contraction ratio for branches */
#define a0 45    /* branching angle from the trunk */
#define a2 45    /* branching angle for lateral axes */
#define d 137.5  /* divergence angle */
#define wr 0.707 /* width decrease rate */

ω : A(1,10)
p1 : A(1,w) : * → !(w)F(1) [&(a0)B(1*r2,w*wr)]/(d)A(1*r1,w*wr)
p2 : B(1,w) : * → !(w)F(1) [-(a2)$C(1*r2,w*wr)]C(1*r1,w*wr)
p3 : C(1,w) : * → !(w)F(1) [(a2)$B(1*r2,w*wr)]B(1*r1,w*wr)

```

Figure 2.6: Examples of the monopodial tree-like structures of Honda [65], generated using L-systems

According to production p_1 , the apex of the main axis A produces an internode F and a lateral apex B in each derivation step. Constants r_1 and r_2 specify contraction ratios for the straight and lateral segments, a_0 and a_2 are branching angles and d is the divergence angle. Module $!(w)$ sets the line width to w , thus production p_1 decreases the width of the daughter segments with respect to the mother segment by the factor $w_r = 0.707$. This constant satisfies a postulate by Leonardo da Vinci [95, page 156], according to which “all the branches of a tree at every stage of its height when put together are equal in thickness to the trunk below them.” In the case where a mother branch of diameter w_1 gives rise to two daughter branches of equal diameter w_2 , this postulate yields the equation $w_1^2 = 2w_2^2$, which gives a value for w_r equal to $w_2/w_1 = 1/\sqrt{2} \approx 0.707$. A general discussion of the relationships between the diameters of the mother and daughter branches is included in the book by Macdonald [94, pages 131–135].

Productions p_2 and p_3 describe subsequent development of the lateral branches. In each derivation step, the straight apex (either B or C) issues a lateral apex of the next order at angle a_2 or $-a_2$ with respect to the mother axis. Two productions are employed to create lateral apices alternately to the left and right. The symbol $\$$ rolls the turtle around its own axis so that vector \vec{L} pointing to the left of the turtle (Section 1.5) is brought to a horizontal position. Consequently, the branch plane is “closest to a horizontal plane,” as required by Honda’s model. From a technical point of view, $\$$ modifies the turtle orientation in space according to the formulae

$$\vec{L} = \frac{\vec{V} \times \vec{H}}{|\vec{V} \times \vec{H}|} \quad \text{and} \quad \vec{U} = \vec{H} \times \vec{L},$$

where vectors \vec{H} , \vec{L} and \vec{U} are the heading, left and up vectors associated with the turtle, \vec{v} is the direction opposite to gravity, and $|\vec{A}|$ denotes the length of vector \vec{A} . The tree-like structures shown in Figure 2.6 were generated using the values of constants listed in Table 2.1, and coincide with the structures presented by Honda.

Figure	r_1	r_2	a_0	a_2
a	0.9	0.6	45	45
b	0.9	0.9	45	45
c	0.9	0.8	45	45
d	0.9	0.7	30	-30

Table 2.1: Constants for the monopodial tree structures in Figure 2.6

Monopodial branching

Branch width

Keeping turtle’s orientation

*Sympodial
branching*

A slightly different L-system, specified in Figure 2.7, captures *sympodial* structures, where both daughter segments form non-zero angles with the mother segment. In this case the activity of the main apex is reduced to the formation of the trunk F and a pair of lateral apices B (production p_1). The subsequent branching pattern is captured by production p_2 . The sample structures in Figure 2.7 were obtained using the constants listed in Table 2.2, and correspond to the models presented by Aono and Kunii.

The L-systems considered so far have been designed in a manner that emphasizes their relation to the models described in the literature. Specifically, all segments are assigned their final length at the time of creation, and no further elongation occurs. As pointed out in Section 1.10.3, similar structures can be obtained by creating new segments of constant length and increasing the lengths of previously created segments by a constant factor in each derivation step. A sample L-system constructed according to this paradigm is given in Figure 2.8.

*Ternary
branching*

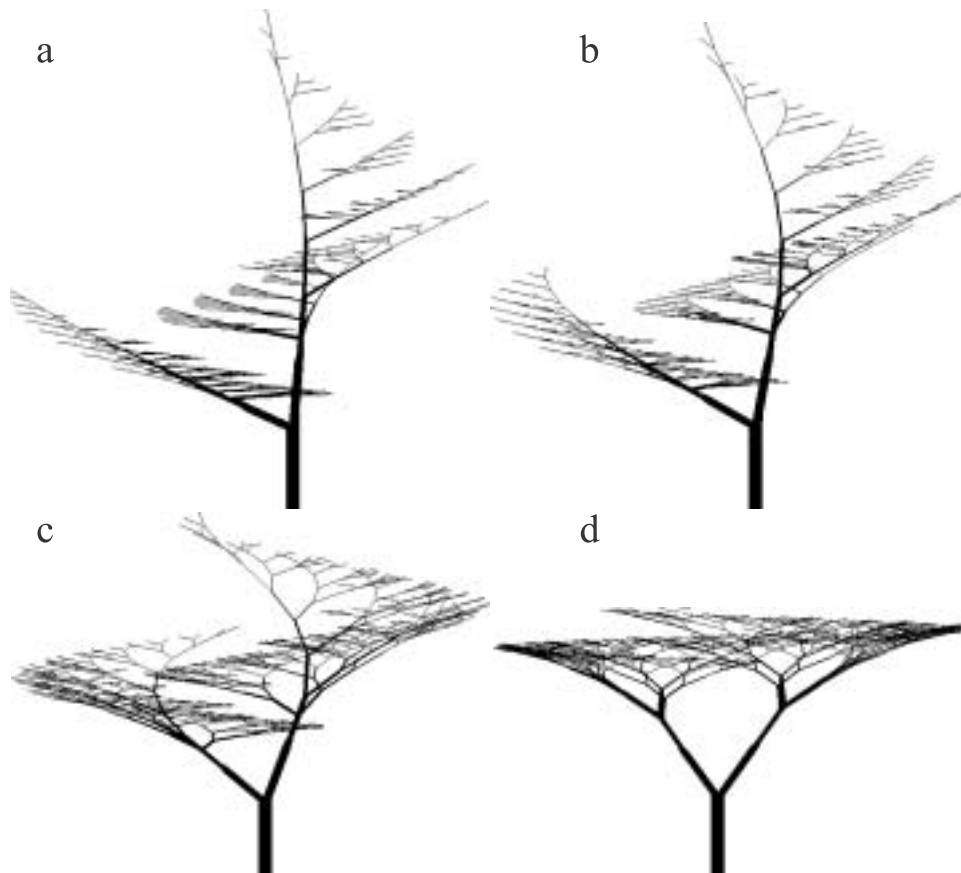
The overall structure of the tree is defined by production p_1 . In each derivation step, apex A produces three new branches terminated by their own apices. Parameter w and constant v_r relate the width of the mother branch w_1 to that of the daughter branches w_2 . According to da Vinci's postulate $w_1^2 = 3w_2^2$, thus $v_r = w_1/w_2 = \sqrt{3} \approx 1.732$. Productions p_2 and p_3 capture the gradual elongation of branches and the increase in their diameter over time.

Tropism

The bending of branches is simulated by slightly rotating the turtle in the direction of a predefined *tropism vector* \vec{T} after drawing each segment (Figure 2.9). The orientation adjustment α is calculated using the formula $\alpha = e |\vec{H} \times \vec{T}|$, where e is a parameter capturing axis susceptibility to bending. This heuristic formula has a physical motivation; if \vec{T} is interpreted as a force applied to the endpoint of vector \vec{H} , and \vec{H} can rotate around its starting point, the torque is equal to $\vec{H} \times \vec{T}$. The parameters relevant to the generation of the tree-like structures in Figure 2.8 are listed in Table 2.3. A more realistic rendering of the tree in Figure 2.8d is presented in Figure 2.10.

Figure	r_1	r_2	a_1	a_2
a	0.9	0.7	5	65
b	0.9	0.7	10	60
c	0.9	0.8	20	50
d	0.9	0.8	35	35

Table 2.2: Constants for the sympodial tree structures in Figure 2.7



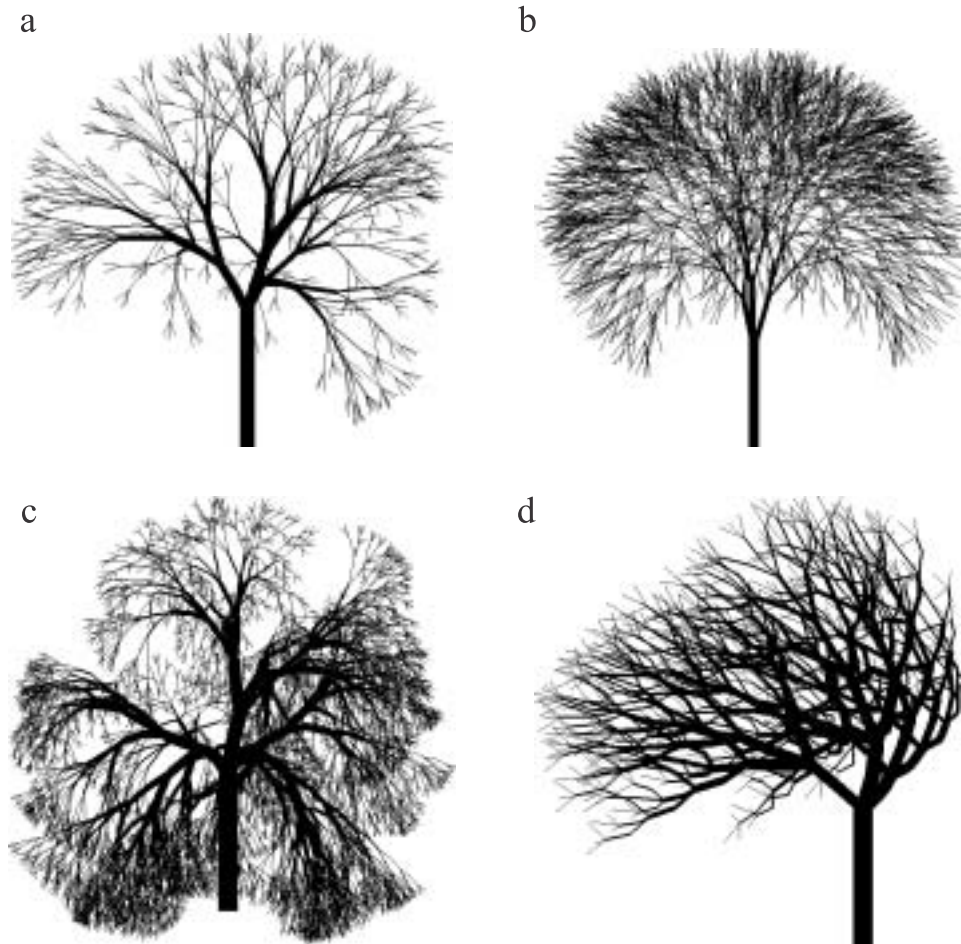
```

n = 10
#define r1 0.9 /* contraction ratio 1 */
#define r2 0.7 /* contraction ratio 2 */
#define a1 10 /* branching angle 1 */
#define a2 60 /* branching angle 2 */
#define w_r 0.707 /* width decrease rate */

ω : A(1,10)
p1 : A(l,w) : * → !(w)F(1) [&(a1)B(l*r1,w*w_r)]
      / (180) [&(a2)B(l*r2,w*w_r)]
p2 : B(l,w) : * → !(w)F(1) [+ (a1)$B(l*r1,w*w_r)]
      [- (a2)$B(l*r2,w*w_r)]

```

Figure 2.7: Examples of the symphydial tree-like structures of Aono and Kunii [2], generated using L-systems



```

#define d1 94.74      /* divergence angle 1 */
#define d2 132.63   /* divergence angle 2 */
#define a 18.95       /* branching angle */
#define lr 1.109    /* elongation rate */
#define vr 1.732   /* width increase rate */

```

```

ω : !(1)F(200)/(45)A
p1 : A : * → !(vr)F(50) [&(a)F(50)A]/(d1)
      [&(a)F(50)A]/(d2) [&(a)F(50)A]
p2 : F(1) : * → F(1*lr)
p3 : !(w) : * → !(w*vr)

```

Figure 2.8: Examples of tree-like structures with ternary branching

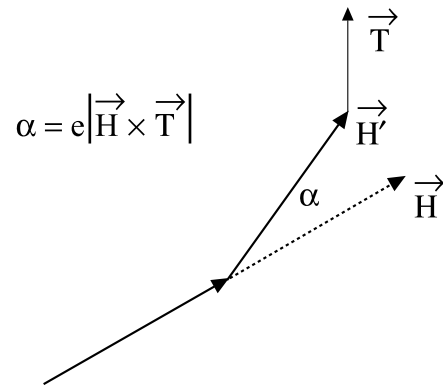


Figure 2.9: Correction α of segment orientation \vec{H} due to tropism \vec{T}

Figure	d_1	d_2	a	l_r	\vec{T}	e	n
a	94.74	132.63	18.95	1.109	0.00,-1.00,0.00	0.22	6
b	137.50	137.50	18.95	1.109	0.00,-1.00,0.00	0.14	8
c	112.50	157.50	22.50	1.790	-0.02,-1.00,0.00	0.27	8
d	180.00	252.00	36.00	1.070	-0.61,0.77,-0.19	0.40	6

Table 2.3: Constants for the tree structures in Figure 2.8



Figure 2.10: *Medicine Lake* by Musgrave *et al.* [101]



Figure 2.11: A surrealistic elevator

Conclusions

The examples given above demonstrate that the tree models of Honda, as well as their derivatives studied by Aono and Kunii, can be expressed using the formalism of L-systems. In a separate study, Shebell [130] also showed that L-systems can be applied to generate the architectural tree models of Hallé, Oldeman and Tomlinson [58]. These results indicate that L-systems may play an important role as a tool for biologically-correct simulation of tree development and synthesis of realistic tree images. However, the tree-like shapes created so far are rather generic (Figure 2.11), and models of particular tree species, directly based on biological data, are yet to be developed. L-systems have found more applications in the domain of realistic modeling of herbaceous plants, discussed in the next chapter.